https://doi.org/10.5194/egusphere-2026-3205
Preprint. Discussion started: 21 July 2026
© Author(s) 2026. CC BY 4.0 License.

China–Korea Linked Typhoons: A transboundary sequential hazard framework for East Asian tropical cyclones

Hana Na[1,2], Woo-Sik Jung[1,2]
[1]Department of Atmospheric Environment and Information Engineering, Inje University, Gimhae 50834, Republic of Korea
[2]Typhoon Ready Center, Inje University, Gimhae 50834, Republic of Korea
Correspondence to: Woo-Sik Jung (wsjung1@inje.ac.kr)

Abstract. Tropical cyclones over the western North Pacific (WNP) are among the most damaging natural hazards in East Asia, yet the transboundary sequential process by which a single typhoon affects China and then Korea has not been quantified. This study proposes the China–Korea Linked Typhoon (CKLT) framework and applies it to 70 years of official records (1949–2018) from the China Meteorological Administration (CMA) and the Korea Meteorological Administration (KMA). A CKLT is defined by three criteria: (i) the same WNP typhoon number appears in both CMA and KMA records; (ii) the China impact onset precedes or coincides with the Korea impact onset; and (iii) the Forecast Window (FW), defined as the interval between the two onsets, does not exceed 14 d. The FW is an observational temporal linkage metric, not a forecast skill measure. The 14 d threshold is jointly supported by Gaussian mixture model decomposition, kernel density estimation, and physical transit-time considerations, with the resulting case count stable across thresholds of 12–19 d. Mann–Kendall analysis revealed asymmetric long-term changes: China-affecting typhoon frequency in the CMA W8 station record increased (+ 0.570 events decade^{-1}, $p = 0.006$; constant-network subset + 0.45 events decade^{-1}, $p = 0.032$) while station-based mean wind and gust decreased; Korea-affecting typhoons in the KMA advisory record showed no frequency trend but exhibited intensification in advisory-based extreme gusts (+ 1.41 m s^{-1} decade^{-1}, $p = 0.022$) and typhoon-conditional precipitation (+ 24.7 mm decade^{-1}, $p < 0.001$). Of the 227 Korea-affecting typhoons, 75 shared a common WNP typhoon number with CMA records and satisfied the sequential onset criterion; applying the 14 d Forecast Window threshold identified 36 (15.9 %) as CKLTs, with the FW distribution adequately represented by a parsimonious gamma model ($\alpha = 1.20$, $\beta = 5.21$; KS $p = 0.258$) and a 6 d median (95 % bootstrap CI [2.95, 6.78] d; B = 5000). These results support the CKLT framework as an observation-based, population-level timing indicator for transboundary typhoon hazard analysis and bilateral disaster-preparedness research, rather than as a deterministic forecast of individual storm impacts.

1 Introduction

Typhoons generated over the western North Pacific (WNP) rank among the most destructive natural hazards in East Asia, causing recurring human casualties and large-scale socioeconomic losses across China, the Korean Peninsula, Japan, and neighbouring regions (Emanuel, 2005; Webster et al., 2005). In China, typhoons cause annual average direct economic losses exceeding USD 28 billion, while in Korea, individual events such as Typhoon Rusa (2002; USD 4.2 billion) and Typhoon

https://doi.org/10.5194/egusphere-2026-3205
Preprint. Discussion started: 21 July 2026
© Author(s) 2026. CC BY 4.0 License.

Maemi (2003; USD 4.8 billion) have inflicted damages comparable to major national disasters. Critically, both Rusa and Maemi first produced measurable impacts across China's coastal provinces before striking Korea within days – a sequential transboundary impact pattern whose systematic structure has not previously been quantified. As individual WNP typhoons traverse the East China Sea–Yellow Sea corridor, they frequently impose sequential hazard impacts on both China and Korea within a matter of days – a transboundary impact structure with direct implications for disaster risk management, preemptive allocation of emergency resources, and observation-based early warning. Despite its practical importance, this sequential impact phenomenon has received limited systematic quantitative attention: existing studies have examined typhoon frequency, intensity, and hazard impacts extensively within individual national domains (Ren et al., 2006; Na and Jung, 2020, 2024), but no quantitative framework has been established to identify and characterise the China–Korea sequential impact structure as an integrated transboundary hazard process.

This gap is increasingly consequential in light of intensifying typhoon-related hazards across East Asia and growing international commitments to multi-hazard early warning systems. The Sendai Framework for Disaster Risk Reduction 2015–2030 (UNDRR, 2015) explicitly identifies the substantial increase in availability of multi-hazard early warning systems as a global target, and the WMO Early Warnings for All initiative further underscores the need for actionable, cross-border warning capability. Yet for East Asian typhoon hazards – where the same storm can sequentially affect multiple countries – no observation-based framework exists to characterise the transboundary timing structure that would enable earlier preparedness across national boundaries. Recent literature has increasingly emphasised that climate hazards often manifest not as independent extreme events confined to single regions, but as compound or cascading processes interconnected across regions and time scales (Zscheischler et al., 2018; Brett et al., 2025). Zscheischler et al. (2020) proposed a typology of compound events – including preconditioned, multivariate, temporally compounding, and spatially compounding types – while Raymond et al. (2020) introduced the concept of connected extreme events, in which physical interactions and societal factors can amplify risk when multiple extreme events are linked. Viewed through this lens, sequential typhoon impacts on China and Korea can be interpreted as a transboundary, temporally connected hazard process in which hazard characteristics evolve continuously in space and time along the storm track. From a disaster risk reduction perspective, such connected hazard chains are particularly significant because the first impact in the sequence – the China landfall – may constitute an observable precursor signal for the subsequent Korea impact, potentially extending the effective preparedness window for downstream emergency managers. The CKLT framework proposed here builds on this compound-event perspective in the East Asian typhoon context.

Long-term changes in WNP typhoon activity further amplify the urgency of a transboundary perspective. The poleward migration of maximum typhoon intensity (Kossin et al., 2014) has progressively increased the exposure of mid-latitude regions such as Korea to intense typhoons, while recent studies have reported increases in rapid intensification frequency and typhoon-related precipitation (Liu and Chan, 2022; Stansfield and Reed, 2023). In addition, accelerating sea surface temperature (SST) warming in the East China Sea and the seas surrounding the Korean Peninsula (Han et al., 2023; Kim et al., 2024) provides a thermodynamic environment that may modulate typhoon intensity, moisture supply, and precipitation structure as storms

https://doi.org/10.5194/egusphere-2026-3205
Preprint. Discussion started: 21 July 2026
© Author(s) 2026. CC BY 4.0 License.

approach Korea. Nevertheless, most existing studies treat China and Korea as separate typhoon impact domains, leaving insufficiently characterised the spatiotemporal linkage structure by which hazard characteristics evolve as a single typhoon sequentially affects both countries along a continuous transboundary storm track. This single-country analytical limitation is itself a barrier to realising the cross-border early warning goals articulated in the Sendai Framework.

These considerations raise a practically important question: do typhoon hazards over China and Korea evolve coherently or asymmetrically when viewed as part of a sequential transboundary impact pathway, and can observed China impact information provide actionable early warning value for Korea? If the same WNP typhoon can first produce measurable impacts in China and then affect Korea within a short, statistically characterisable interval – as the 36 CKLT cases identified in this study demonstrate, with a median sequential impact interval of approximately 6 d – the initial China impact may function as an observation-based precursor signal for subsequent Korea-related typhoon risk, complementing numerical forecast guidance and supporting earlier situational awareness for disaster managers (Kooshki Forooshani et al., 2024). However, such a possibility cannot be adequately evaluated within single-country analytical frameworks. A transboundary framework is therefore needed to identify linked China–Korea typhoon cases, quantify their sequential timing, and characterise how associated hazard indicators differ between the two countries.

We therefore propose and evaluate the China–Korea Linked Typhoon (CKLT) framework using 70 years of official observational records from both countries. A CKLT is defined as a WNP typhoon satisfying three criteria: (i) the same WNP typhoon number (YYYYNN) is confirmed in both CMA and KMA official records; (ii) the China impact onset (ChnStart) occurs earlier than or at the same time as the Korea impact onset (KorStart); and (iii) the Forecast Window (FW), defined as the time interval from ChnStart to KorStart, is 14 d or less. The FW is introduced as a temporal linkage metric that characterises the China-to-Korea sequential impact interval and provides a potential observation-based timing indicator for probabilistic early warning in Korea.

Framed within the natural-hazards and disaster-risk research perspective central to this journal, this study quantifies a transboundary sequential hazard process across two national impact domains in East Asia. The proposed CKLT framework reframes paired China–Korea typhoon impacts as a connected hazard chain rather than two independent national events, providing an observational basis that can inform cross-border early warning practice and probabilistic regional risk assessment consistent with disaster risk reduction goals.

This study makes three main contributions to transboundary typhoon hazard science. First, it quantitatively characterises long-term changes in typhoon frequency and hazard indicators over China and Korea using a unified analytical framework for 1949–2018, revealing asymmetric trends that single-country assessments cannot fully capture. Second, it introduces the CKLT framework to identify sequential China–Korea typhoon impacts, quantify the statistical distribution of the Forecast Window, and evaluate its robustness using distributional analysis and bootstrap resampling. Third, it reframes East Asian typhoon hazards as sequential transboundary risk processes rather than isolated national events, thereby providing an observation-based foundation for probabilistic regional risk assessment and early warning that complements existing numerical forecast systems.

https://doi.org/10.5194/egusphere-2026-3205
Preprint. Discussion started: 21 July 2026
© Author(s) 2026. CC BY 4.0 License.

2 Data and methods

2.1 China typhoon data: CMA Beaufort-8 (W8) dataset

China typhoon impact data were derived from the China Meteorological Administration (CMA) Beaufort scale 8 or above dataset (W8; sustained wind speed ≥ 17.2 m s⁻¹), compiled from official station observations (Ying et al., 2014). The dataset covers 184 meteorological stations across China for 1949–2018 and provides, for each typhoon, station-level Bft ≥ 8 onset and end dates, maximum wind speed, maximum gust speed, and daily precipitation. The W8 dataset is based on the CMA official operational criterion for identifying typhoon impacts in China and has been widely used in Chinese typhoon hazard studies (Ren et al., 2006). In this study, a typhoon was classified as a China-affecting event when at least one of the 184 stations recorded Bft ≥ 8 conditions, corresponding to the minimum operational detection criterion used in Chinese disaster management practice. Typhoon identification followed the WNP integrated numbering system (YYYYNN), which served as the common identifier for linking cases across the JMA Best Track, CMA, and KMA datasets.

The W8 station network covers a broad geographic domain across China, spanning approximately 19°N to 49°N and 76°E to 132°E. About half of the 184 stations (92 stations, 50 %) are located within the principal typhoon impact zone of eastern and southern China (18°–41°N, 105°–125°E), including 38 stations along the southern coast (≤30°N) and 28 stations along the central and northern coast (30°–41°N). This concentration of stations along the typhoon-prone seaboard means that any landfalling typhoon producing Bft ≥ 8 winds at the coast is likely to be detected by at least one constituent station throughout the study period. We note that the number of operational CMA stations contributing to the W8 record was not strictly constant across 1949–2018; the network expanded gradually as the national observational system was consolidated. However, the W8 criterion is intensity-based (sustained wind ≥ 17.2 m s⁻¹) rather than count-based: a newly added station contributes to the impact record only if it observes Bft ≥ 8 winds during a passing typhoon, which is a stricter requirement than mere station existence. The potential influence of this network non-stationarity on the long-term frequency trend reported in Sect. 3.1 is therefore expected to be partial rather than dominant and is discussed further in Sect. 4.5.

2.2 Korea typhoon data: KMA official typhoon impact list

Korea typhoon impact data were obtained from the Korea Meteorological Administration (KMA) official typhoon impact list for 1949–2018, which includes 227 Korea-affecting typhoon cases. KMA defines a Korea-affecting typhoon as a typhoon that enters the emergency zone north of 28° N and west of 128° E while a typhoon special advisory — either a typhoon watch or warning — is in effect (Na and Jung, 2020). Each record includes the typhoon number, impact period, maximum wind speed, maximum instantaneous wind speed, accumulated precipitation, and minimum sea-level pressure. KMA typhoon numbers in YYXX format were converted to the WNP integrated numbering system (YYYYNN) to ensure consistency with the CMA and JMA datasets, and all matched cases were manually verified. The KMA emergency-zone and advisory-issuance criteria have been applied consistently throughout the 1949–2018 record, and the 227 Korea-affecting cases reflect the operational

https://doi.org/10.5194/egusphere-2026-3205
Preprint. Discussion started: 21 July 2026
© Author(s) 2026. CC BY 4.0 License.

definition currently in use by KMA. The Korea-affecting typhoon frequency reported in this study should therefore be interpreted as the population of typhoons that satisfied the KMA advisory criterion, rather than as a count of all typhoons that physically passed within the emergency zone.

The typhoon impact definitions used by CMA and KMA are based on different operational criteria: CMA applies a station-based wind threshold (Bft ≥ 8 at any of the constituent CMA stations), whereas KMA applies emergency-zone entry combined with typhoon-advisory issuance. The CMA criterion is therefore an intensity threshold applied to point observations, while the KMA criterion is a combined geographic and advisory-based criterion applied at the national operational level. This heterogeneity reflects the operational nature of national typhoon impact records and is inherent to the use of officially recognised national impact archives rather than a methodological choice of this study. Rather than imposing a single physically equivalent intensity threshold across countries, this study retained each country's official operational definition because the CKLT framework is designed to link nationally recognised operational impact events as documented by the responsible national meteorological services. Consequently, absolute cross-national intensity comparisons were not attempted; instead, the analysis focused on event linkage, sequential timing, and within-country hazard characteristics, with cross-country comparisons interpreted in terms of trend direction and relative behaviour rather than absolute magnitudes (Sect. 3.2).

The study period ends in 2018, corresponding to the latest year for which both the CMA W8 station record and the KMA official typhoon impact list were available to the authors at the time of analysis.

2.3 Supplementary data

Annual WNP typhoon genesis counts were computed from the JMA Best Track dataset (Japan Meteorological Agency, 2019) by counting tropical storms and stronger systems with maximum wind speed ≥ 17.2 m s^{-1} in each year. These counts were used to assess long-term changes in the overall WNP typhoon activity background during the study period.

2.4 Mann–Kendall test and Sen's slope

Monotonic long-term trends were analysed using the non-parametric Mann–Kendall (MK) test (Mann, 1945; Kendall, 1975), which does not require a normality assumption and is relatively robust to outliers, making it widely applicable to climate and hydrological time series (Wilks, 2011). A two-tailed significance level of $\alpha = 0.05$ was adopted. Trend magnitudes were quantified using Sen's slope estimator (Sen, 1968) and expressed as decadal rates. Because serial correlation can affect MK test results (Hamed and Rao, 1998; Yue and Wang, 2004), Ljung–Box tests were applied to the key annual time series analysed in this study. No statistically significant autocorrelation was detected at the 10 % level, and pre-whitening was therefore not applied.

https://doi.org/10.5194/egusphere-2026-3205
Preprint. Discussion started: 21 July 2026
© Author(s) 2026. CC BY 4.0 License.

2.5 CKLT definition and identification

To identify the sequential impact structure in which the same typhoon affects China and Korea in succession, we define a China–Korea Linked Typhoon (CKLT) as a WNP typhoon satisfying the following three criteria. First, for event consistency, the same WNP typhoon number (YYYYNN) must be confirmed in both the CMA W8 dataset and the KMA official typhoon impact list. Second, for sequential impact, the China impact onset date (ChnStart) must occur earlier than or on the same date as the Korea impact onset date (KorStart), such that ChnStart ≤ KorStart. Cases in which the Korea impact precedes the China impact were excluded. Third, for temporal linkage, the Forecast Window, defined as

$$\mathrm{FW} = \mathrm{KorStart} - \mathrm{ChnStart}, \quad (1)$$

where ChnStart and KorStart refer to the same WNP typhoon number satisfying criterion (i) and the ordering ChnStart ≤ KorStart satisfying criterion (ii), must not exceed 14 d. FW is therefore defined only for non-negative lags between paired CMA–KMA records and is undefined for unmatched or reverse-ordered cases.

The term 'Forecast Window' (FW) is used in the operational sense of a planning window — the time available to Korean disaster-response authorities for cross-border preparedness once a China impact has been observed — rather than in the forecast-skill sense of a numerical-prediction lead time. The FW is computed entirely from post-event observational records of both national meteorological services and does not involve any forecast model output, advisory-issuance timing, or predicted variable. We retain the present terminology because the operational-planning sense of 'window' is central to the conceptual contribution of this study, and because no shorter alternative captures the same operational meaning. The reader is asked to interpret FW throughout as a statistical characterisation of historical inter-country impact lags, not as a measure of forecast performance.

Because both the CMA W8 and KMA official impact records are provided at daily resolution, ChnStart, KorStart, and FW were calculated using calendar dates. Cases with FW = 0 were retained because they indicate same-day China and Korea impact onsets within the resolution of the source records. The 14 d threshold was adopted as a conservative pre-analysis inclusion criterion based jointly on three lines of evidence: physical travel-time considerations, Gaussian mixture model decomposition of the same-number CMA–KMA pair distribution (Sect. 3.3.1), and kernel density estimation of the same distribution (Sect. 3.3.2), and the need to exclude temporally disconnected events. The convergence of these three independent criteria on a comparable cut-off, together with the limited sensitivity of the resulting case count across thresholds of 5–30 d (Sect. 3.3.3), supports the use of 14 d as an inclusive upper bound rather than an arbitrary choice. Given a representative China–Korea travel distance of approximately 500–1000 km and typical typhoon translation speeds of 15–25 km h^{-1}, direct transit times are approximately 1–3 d. When accounting for typical CMA impact durations of 1–5 d and the possibility of slow-moving or recurving tracks, the physically plausible sequential impact time scale can extend beyond the direct transit time. Therefore, FW ≤ 14 d was used as an inclusive upper bound for identifying linked events. Subsequent FW analysis focuses on the observed distribution and its median-scale timing rather than assuming that all events near the threshold have equal operational relevance.

https://doi.org/10.5194/egusphere-2026-3205
Preprint. Discussion started: 21 July 2026
© Author(s) 2026. CC BY 4.0 License.

The FW functions as an observational temporal linkage metric for quantifying the China-to-Korea sequential impact structure at the population level. It is not used as a direct predictor of hazard intensity, a measure of numerical-prediction lead time, or a deterministic forecast of individual typhoon impacts.

2.6 Distributional analysis of the Forecast Window

The statistical characteristics of the FW were analysed to evaluate whether the sequential China-to-Korea impact interval exhibits a coherent probabilistic timing structure. Because the FW is a non-negative waiting-time variable and may exhibit right-skewed behaviour, a gamma distribution was used as a parametric model for the FW distribution. FW = 0 cases were retained in the gamma fitting as the fitted shape parameter ($\alpha = 1.20$) yields a finite density at the origin under the standard gamma parameterisation. The shape and scale parameters were estimated from the observed CKLT sample, and goodness of fit was evaluated using the Kolmogorov–Smirnov (KS) test. The fitted distribution was used to characterise the central tendency and uncertainty of the FW, with emphasis on median-scale timing rather than rare tail behaviour.

To assess the sensitivity of the FW threshold, a two-component Gaussian mixture model (GMM) was fitted to all same-number China–Korea pairs to examine the separation between short- and long-FW groups (McLachlan and Peel, 2000). Kernel density estimation (KDE) was also used to identify local minima in the FW distribution (Silverman, 1986).

To assess the sampling uncertainty associated with the limited number of CKLT cases, non-parametric bootstrap resampling was conducted using 5000 resamples (Efron and Tibshirani, 1993). For each bootstrap sample, the FW distribution parameters and median FW were recalculated, and the 95 % confidence interval (CI) was estimated from the empirical bootstrap distribution. The bootstrap analysis was used as a robustness check for the stability of the central FW estimate under the observed sample, not as a substitute for independent validation.

3 Results

3.1 Long-term changes in typhoon frequency

Table 1 summarises the Mann–Kendall test results for WNP typhoon genesis and China/Korea-affecting typhoon frequency during 1949–2018. Total WNP typhoon genesis shows no statistically significant long-term trend ($p = 0.299$). In contrast, China-affecting typhoon frequency as recorded by the CMA W8 station network increases significantly, with a Sen's slope of + 0.570 events decade^{-1} ($p = 0.006$). This trend is robust to expansion of the CMA observational network: the number of stations actually contributing to the W8 record each year shows no significant long-term trend (Mann–Kendall $p = 0.37$), and a constant-network subset using only the 22 stations operational during 1949–1955 yields a comparable positive slope (+ 0.45 events decade^{-1}, $p = 0.032$; see Sect. 4.5). The ratio of China-affecting typhoons to total WNP genesis also shows a statistically significant increasing trend (Sen's slope = + 0.022 decade^{-1}, $p = 0.003$), suggesting that the proportion of WNP typhoons affecting China has gradually increased over the study period. Korea-affecting typhoon frequency in the KMA advisory record

https://doi.org/10.5194/egusphere-2026-3205
Preprint. Discussion started: 21 July 2026
© Author(s) 2026. CC BY 4.0 License.

shows no significant long-term trend ($p = 0.559$). These contrasting results suggest that regional impact frequency can evolve differently from basin-wide WNP genesis activity.

https://doi.org/10.5194/egusphere-2026-3205
Preprint. Discussion started: 21 July 2026
© Author(s) 2026. CC BY 4.0 License.

Table 1. Mann–Kendall test results for annual WNP typhoon genesis and China/Korea-affecting typhoon frequency during 1949–2018. Sen's slopes are expressed per decade; frequency variables are in events decade^{-1}, whereas the China/WNP ratio is in ratio decade^{-1}. ns indicates not significant; * $p < 0.05$; ** $p < 0.01$. Mean values during the study period: WNP total = 26.2 events yr^{-1}; China = 10.4 events yr^{-1}; China/WNP ratio = 0.40; Korea = 3.2 events yr^{-1}.

Variable	Sen's slope (decade^{-1})	p-value
WNP total genesis	+ 0.001	0.299
China-affecting typhoons (Bft ≥ 8, ≥ 17.2 m s^{-1})	+ 0.570	0.006
China/WNP ratio	+ 0.022	0.003
Korea-affecting typhoons (emergency zone + typhoon advisory)	+ 0.001	0.559

https://doi.org/10.5194/egusphere-2026-3205
Preprint. Discussion started: 21 July 2026
© Author(s) 2026. CC BY 4.0 License.

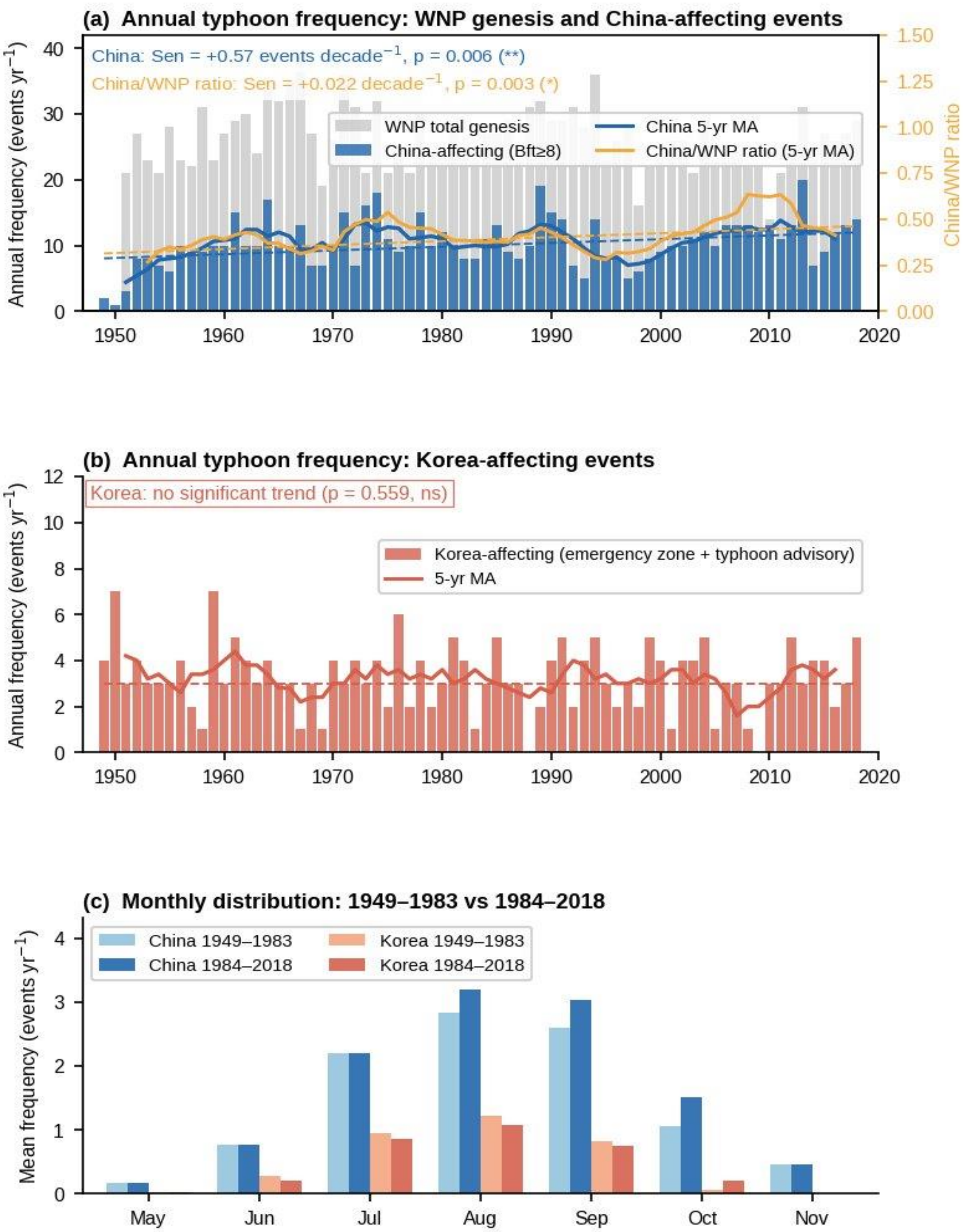

Figure 1. Annual typhoon frequency during 1949–2018. (a) WNP total genesis (grey bars), China-affecting typhoons (blue bars; Bft ≥ 8, ≥ 17.2 m s⁻¹), and the China/WNP ratio (orange line). (b) Korea-affecting typhoons based on the KMA emergency-zone and typhoon-advisory criterion. Thick lines indicate 5 yr moving averages, and dashed lines indicate Sen's slopes. (c) Monthly distributions of China- and Korea-affecting typhoons for 1949–1983 and 1984–2018.

https://doi.org/10.5194/egusphere-2026-3205
Preprint. Discussion started: 21 July 2026
© Author(s) 2026. CC BY 4.0 License.

Figure 1a illustrates the interannual variability of WNP genesis and China-affecting typhoon frequency. While total WNP genesis exhibits strong year-to-year variability without a significant long-term trend, China-affecting typhoon frequency increases over the study period. The China/WNP ratio likewise shows a significant increasing trend (Sen's slope = + 0.022 decade^{-1}, p = 0.003), indicating that a growing proportion of WNP typhoons has been affecting China over the 70 yr record. Korea-affecting typhoons (Fig. 1b) exhibit pronounced interannual variability but no significant long-term directional trend, contrasting with the significant increases in both China-affecting frequency and the China/WNP ratio. Because the CMA W8 dataset is based on station-level impact records, the sensitivity of the China-affecting frequency trend to changes in observational network coverage is examined explicitly in Sect. 4.5; the trend remains positive and statistically significant under a constant-network subset.

Monthly distributions (Fig. 1c) show that both China and Korea typhoon impacts are concentrated in July–September, with maxima in August–September. In the latter subperiod (1984–2018), China-affecting typhoon frequency is relatively higher in September–October than in the earlier subperiod (1949–1983), suggesting a possible late-season redistribution of China impacts. Korea-affecting events remain concentrated mainly in August–September in both subperiods.

3.2 Long-term changes in typhoon intensity: asymmetric patterns

Table 2 presents the MK test results for key typhoon intensity and hazard-related variables in the China and Korea impact records during 1949–2018. Because the CMA and KMA records are based on different operational definitions and variable availability, cross-country comparisons are interpreted in terms of trend direction and relative hazard characteristics rather than absolute magnitudes. Station-based mean maximum wind speed of China-affecting typhoons in the CMA W8 record decreased significantly (Sen's slope = − 0.51 m s^{-1} decade^{-1}, p = 0.001), as did station-based mean maximum gust (Sen's slope = − 0.63 m s^{-1} decade^{-1}, p = 0.001; Fig. 2a and b). Mean maximum wind speed of Korea-affecting typhoons in the KMA advisory record showed no significant long-term change (p = 0.870), but the annual extreme gust of Korea-affecting typhoons increased significantly (Sen's slope = + 1.41 m s^{-1} decade^{-1}, p = 0.022; Fig. 2b). These results indicate that station-based average wind characteristics are weakening over China while advisory-based extreme gust characteristics are intensifying over Korea.

https://doi.org/10.5194/egusphere-2026-3205
Preprint. Discussion started: 21 July 2026
© Author(s) 2026. CC BY 4.0 License.

Table 2. Mann–Kendall test results for typhoon intensity and hazard-related variables during 1949–2018. Sen's slopes are expressed per decade. Variables marked as N/A for China were not available in the CMA W8 dataset and were therefore not analysed. ns = not significant; * $p < 0.05$; ** $p < 0.01$; *** $p < 0.001$.

Variable	Sen's slope (decade^{-1})	p-value	Country
Mean max. wind speed (m s^{-1})	− 0.51 **	0.001	China
Mean max. wind speed (m s^{-1})	− 0.05 ns	0.870	Korea
Mean max. gust (m s^{-1})	− 0.63 **	0.001	China
Annual extreme gust (m s^{-1})	+ 1.41 *	0.022	Korea
Mean accumulated precipitation (mm)	+ 42.1 **	0.005	China
Mean accumulated precipitation (mm)	+ 24.7 ***	< 0.001	Korea
Annual extreme precipitation (mm)	+ 148.1 **	0.004	China
Annual extreme precipitation (mm)	+ 41.4 ***	< 0.001	Korea
Mean min. sea-level pressure (hPa)	—	—	China (N/A)
Mean min. sea-level pressure (hPa)	− 0.79 *	0.039	Korea
Mean impact duration (d)	—	—	China (N/A)
Mean impact duration (d)	− 0.073 *	0.043	Korea

https://doi.org/10.5194/egusphere-2026-3205
Preprint. Discussion started: 21 July 2026
© Author(s) 2026. CC BY 4.0 License.

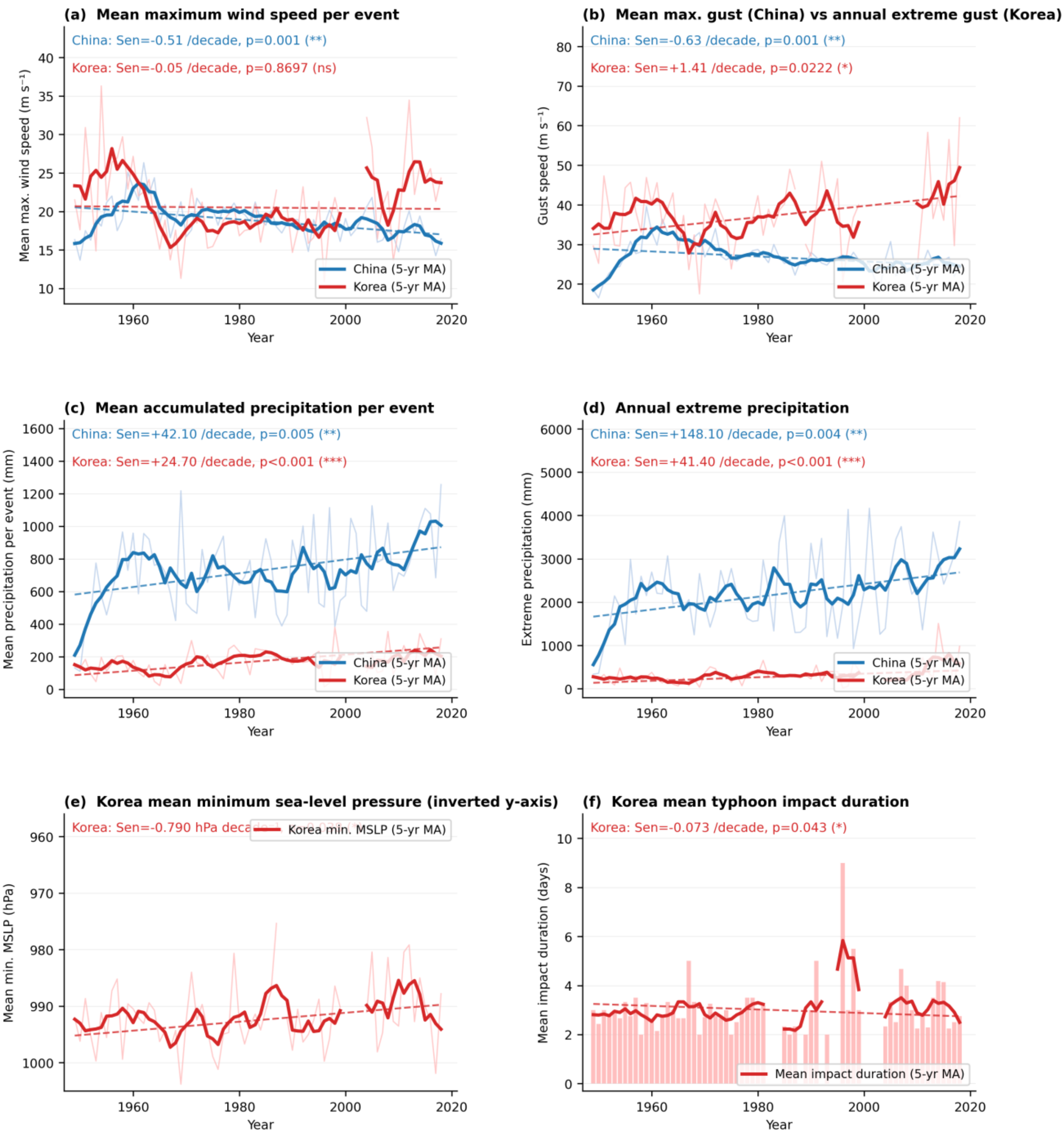

Figure 2. Long-term changes in typhoon intensity and hazard-related variables during 1949–2018. (a) Mean maximum wind speed per event. (b) Mean maximum gust for China-affecting typhoons and annual extreme gust for Korea-affecting typhoons. (c) Mean accumulated precipitation per event. (d) Annual extreme precipitation. (e) Mean minimum sea-level pressure for Korea-affecting typhoons; the y-axis is inverted so that lower pressure values appear higher. (f) Mean impact duration for Korea-affecting typhoons. Blue indicates China-affecting typhoons, and red indicates Korea-affecting typhoons. Thick lines indicate 5 yr moving averages, and dashed lines indicate Sen's slopes.

https://doi.org/10.5194/egusphere-2026-3205
Preprint. Discussion started: 21 July 2026
© Author(s) 2026. CC BY 4.0 License.

Typhoon-conditional precipitation increased over both countries. Mean accumulated typhoon-conditional precipitation of China-affecting typhoons increased by + 42.1 mm decade⁻¹ ($p = 0.005$), and the annual maximum typhoon-conditional precipitation also increased significantly (Sen's slope = + 148.1 mm decade⁻¹, $p = 0.004$; Fig. 2c and d). Korea likewise showed significant increases in both mean accumulated typhoon-conditional precipitation (Sen's slope = + 24.7 mm decade⁻¹, $p < 0.001$) and annual maximum typhoon-conditional precipitation (Sen's slope = + 41.4 mm decade⁻¹, $p < 0.001$). The intensification of Korea typhoon-conditional precipitation without a corresponding increase in event frequency suggests that precipitation amounts per Korea-affecting event have increased over time.

Synthesising Fig. 2, China-affecting typhoons exhibit weakening station-based average wind and gust characteristics while Korea-affecting typhoons exhibit intensifying advisory-based extreme gust and typhoon-conditional precipitation — a contrasting asymmetric pattern as captured by the respective national operational records. The simultaneous weakening of station-based average intensity in the CMA W8 record and the intensification of extreme hazard characteristics in the advisory-based KMA record suggests that operationally documented typhoon hazard indicators can show different long-term behaviour across neighbouring East Asian impact domains, despite the absence of a significant increasing trend in total WNP genesis. The average minimum sea-level pressure of Korea-affecting typhoons in the KMA advisory record showed a significant decreasing trend (Sen's slope = − 0.79 hPa decade⁻¹, $p = 0.039$), and mean impact duration decreased slightly (Sen's slope = − 0.073 d decade⁻¹, $p = 0.043$; Fig. 2e and f), though these variables were unavailable from CMA data for cross-national comparison.

3.3 China–Korea Linked Typhoons: sequential timing and distributional characteristics

The asymmetric frequency and hazard-related changes identified in Sects. 3.1 and 3.2 motivate an examination of whether a subset of WNP typhoons sequentially affects both China and Korea within the official impact records of the two national meteorological services. Applying the CKLT criteria defined in Sect. 2.5 to the full 1949–2018 record, 75 typhoons were found to share a verified WNP number with CMA records and to satisfy the sequential onset criterion (ChnStart ≤ KorStart; Table 3). These sequential same-number pairs accounted for 33.0 % of the 227 Korea-affecting typhoons in the KMA record. Applying the additional FW ≤ 14 d threshold yielded 36 confirmed CKLTs, equivalent to 15.9 % of all Korea-affecting typhoons and 48.0 % of the sequential same-number candidate pairs. The remaining 39 sequential same-number pairs had FW > 14 d and were therefore not classified as CKLTs. At the population level, approximately one in six Korea-affecting typhoons was preceded by or coincident with a documented China impact within the defined FW, indicating that China–Korea sequential impacts are recurrent rather than isolated occurrences in the historical WNP typhoon-impact record. These proportions are retrospective classification statistics and should not be interpreted as real-time conditional probabilities of Korea impact following an observed China impact.

https://doi.org/10.5194/egusphere-2026-3205
Preprint. Discussion started: 21 July 2026
© Author(s) 2026. CC BY 4.0 License.

Table 3. Classification summary of China–Korea Linked Typhoons (CKLTs) during 1949–2018. Percentages in the third column are relative to all KMA Korea-affecting typhoons during 1949–2018 (n = 227), whereas percentages in the fourth column are relative to the verified sequential same-number CMA–KMA pairs (n = 75). Rows are hierarchical and should not be summed directly. ChnStart and KorStart denote the first recorded China and Korea impact dates, respectively.

Classification item	n	% of KMA cases	% of sequential pairs	interpretation
KMA Korea-affecting typhoons	227	100.0	-	Official KMA Korea-affecting typhoon cases during 1949–2018
Sequential same-number CMA-KMA pairs	75	33.0	100.0	Verified same WNP number and ChnStart ≤ KorStart
Confirmed CKLTs	36	15.9	48.0	Sequential same-number pair with FW ≤ 14 d
Sequential pairs outside CKLT threshold	39	17.2	52.0	Sequential same-number pair with FW > 14 d
Non-CKLT Korea-affecting typhoons	191	84.1	-	KMA cases not classified as CKLT, including 152 cases with no verified same-number CMA pair or with reverse onset order

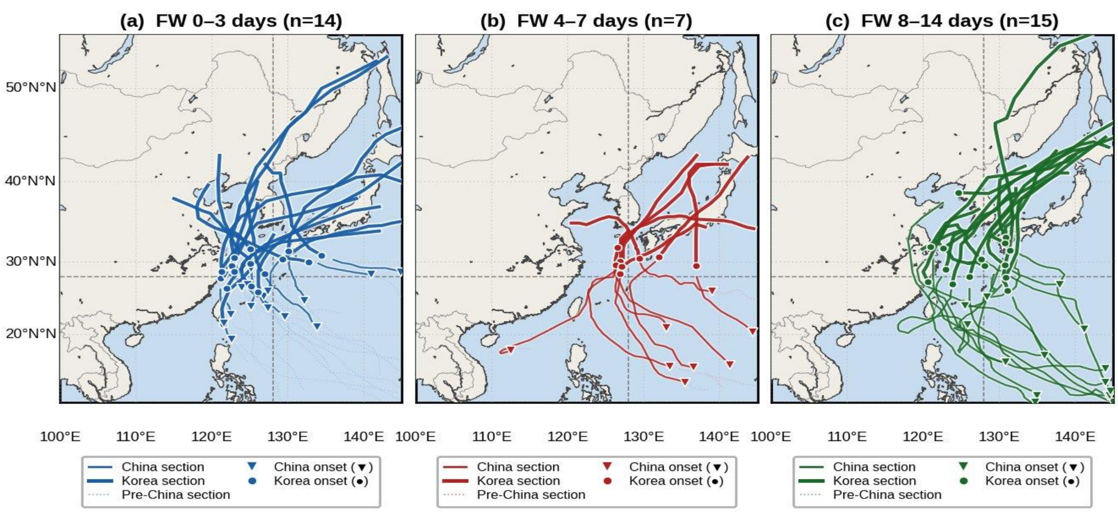

Figure 3. JMA Best Track trajectories of the 36 CKLT cases during 1949–2018, grouped by FW bin: (a) FW 0–3 d (n = 14), (b) FW 4–7 d (n = 7), and (c) FW 8–14 d (n = 15). Triangles denote China impact onset, and circles denote Korea impact onset. Line styles distinguish the pre-China, China-impact, and Korea-impact portions of each track.

https://doi.org/10.5194/egusphere-2026-3205
Preprint. Discussion started: 21 July 2026
© Author(s) 2026. CC BY 4.0 License.

The 36 CKLT Best Track trajectories (Fig. 3), colour-coded by FW bin, show that confirmed CKLT cases generally involve north-eastward movement from south-eastern China, the northern East China Sea, or adjacent coastal waters toward the Korean Peninsula. FW 0–3 d cases (n = 14) tend to follow relatively short and direct pathways along the eastern China coast, the Yellow Sea, or the East China Sea. FW 4–7 d cases (n = 7) include north-eastward recurving tracks through the East China Sea and Yellow Sea. FW 8–14 d cases (n = 15) include longer pathways and more pronounced recurvature in several cases, including tracks passing south of Japan before approaching Korea. These patterns suggest that longer FW cases may be associated with more complex track evolution and mid-latitude steering influences, although process-level attribution requires additional dynamical analysis. Sequential China-to-Korea impacts are nevertheless observed across all FW bins.

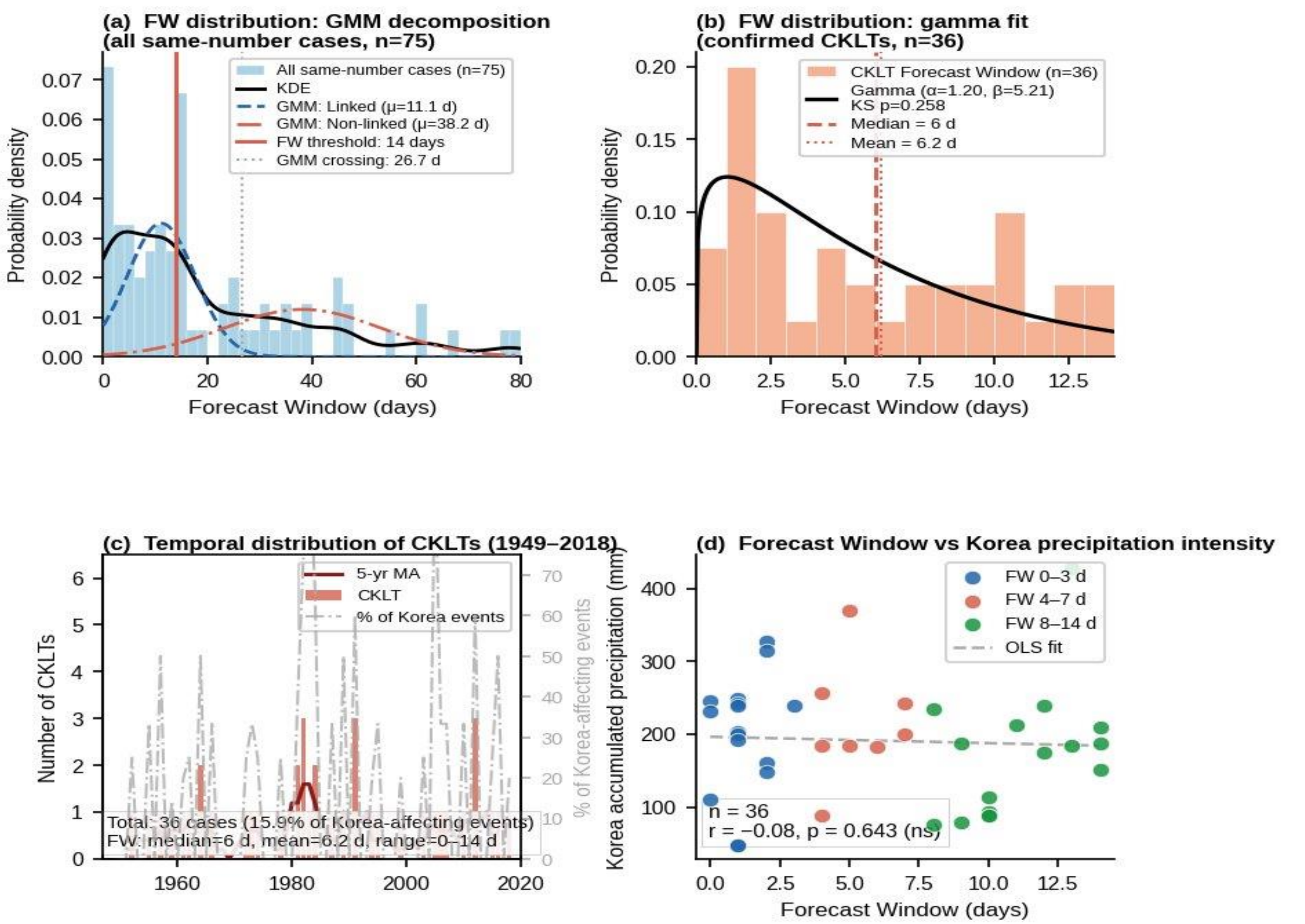

Figure 4. Statistical analysis of the CKLT Forecast Window (FW). (a) FW distribution for all sequential same-number China–Korea pairs satisfying ChnStart ≤ KorStart (n = 75), with KDE and a two-component GMM. Vertical lines indicate the 14 d CKLT threshold and the GMM component crossing point. (b) FW distribution for confirmed CKLT cases (n = 36), with a fitted gamma distribution (α = 1.20, β = 5.21; KS p = 0.258). Bootstrap uncertainty is summarized in Table 4. (c) Annual CKLT counts during 1949–2018. (d) Scatterplot of FW versus Korea accumulated precipitation.

https://doi.org/10.5194/egusphere-2026-3205
Preprint. Discussion started: 21 July 2026
© Author(s) 2026. CC BY 4.0 License.

The choice of the FW ≤ 14 d threshold is consistent with the empirical FW distribution shown in Fig. 4. A two-component GMM fitted to all same-number China–Korea pairs (n = 75) separates a short-FW component (μ_1 = 11.1 d) from a long-FW component (μ_2 = 38.2 d), with a component crossing point at approximately 26.7 d (Fig. 4a). KDE also indicates a local density minimum near 14–16 d, suggesting an empirical separation between short-interval and long-interval same-number pairs. The FW ≤ 14 d criterion therefore provides a conservative threshold that remains well below the GMM crossing point while retaining cases within the short-interval portion of the distribution. Sensitivity analysis across threshold values from 5 to 30 d showed a relatively stable range around 12–19 d, corresponding to 33–37 CKLT cases, indicating that case identification is not highly sensitive to the exact threshold.

For the confirmed CKLT cases, the FW distribution was described using a parsimonious gamma model (α = 1.20, β = 5.21; KS p = 0.258; Fig. 4b). Because FW is recorded in whole calendar days, FW = 0 cases represent same-calendar-day impacts rather than exact zero-duration physical lags. The gamma model is therefore used as a descriptive approximation to the empirical daily FW distribution, not as a literal continuous-time generating process at sub-daily resolution. The fitted distribution indicates that the FW is concentrated within the first one to two weeks, with a median of approximately 6 d. Bootstrap resampling (B = 5000) produced parameter estimates close to the original values (α_boot = 1.29 ± 0.29; β_boot = 5.07 ± 1.33 d; Table 4). The 95 % CIs were α ∈ [0.85, 1.97] and β ∈ [2.88, 8.10] d, with the implied median FW within [2.95, 6.78] d. The bootstrap mean of the resampled median (4.70 d) is slightly lower than the point estimate (6.0 d), reflecting the discrete and slightly skewed sampling distribution of the median in a small (n = 36), right-skewed sample; the original-sample point estimate of 6 d remains the central inference, while the bootstrap interval characterises sampling uncertainty around it. These results indicate that the week-scale central tendency of the FW is statistically stable under resampling, despite substantial event-to-event variability across the 36 CKLT cases.

https://doi.org/10.5194/egusphere-2026-3205
Preprint. Discussion started: 21 July 2026
© Author(s) 2026. CC BY 4.0 License.

Table 4. Non-parametric bootstrap results for the gamma fit of the CKLT Forecast Window distribution (n = 36; B = 5000). α and β denote the shape and scale parameters of the gamma distribution, respectively. Bootstrap means and standard deviations were computed from 5000 resamples. Confidence intervals represent empirical 95 % bootstrap intervals.

Parameter	Point estimate	Bootstrap mean	Bootstrap SD	95 % CI
α (shape)	1.20	1.29	0.29	[0.85, 1.97]
β (scale, d)	5.21	5.07	1.33	[2.88, 8.10]
Distribution mean, αβ (d)	6.25	6.26	0.95	[4.54, 8.25]
Median (d)	6.0	4.70	0.98	[2.95, 6.78]

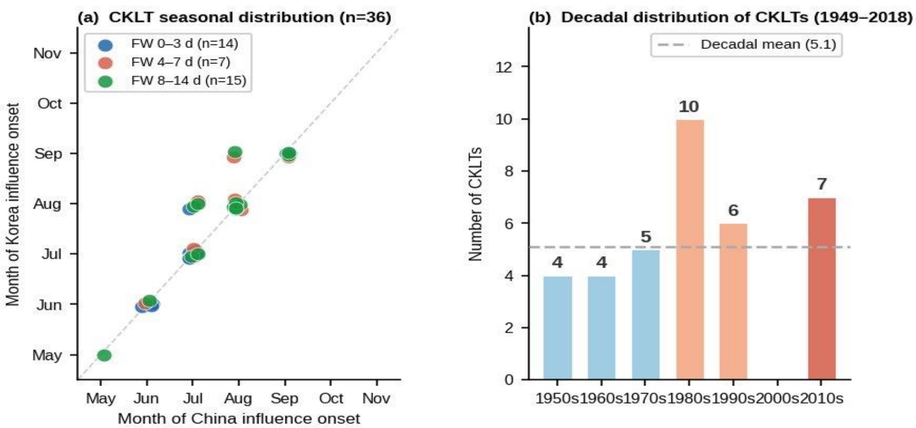

Figure 5. Distributional characteristics of CKLT cases during 1949–2018. (a) Month of China impact onset versus month of Korea impact onset, colour-coded by FW bin. (b) CKLT counts by decade-like period. The dashed line indicates the mean count across displayed period bins. The 2010s bin covers 2010–2018 only.

CKLTs occurred throughout the 70 yr study period without a statistically significant long-term trend (p = 0.899; Fig. 4c) and were concentrated in July–September (Fig. 5a). The decadal distribution (Fig. 5b) shows a relative peak in the 1980s and a relative minimum in the 2000s. However, given the absence of a significant long-term trend, these decadal fluctuations are interpreted as falling within the range of interannual-to-decadal variability.

The linear relationship between FW and Korea typhoon-conditional accumulated precipitation was not statistically significant (r = − 0.08, p = 0.643; Fig. 4d). This result supports the interpretation that FW is an observational temporal linkage metric rather than a direct predictor of hazard intensity at the individual-event level. Actual Korea-related hazard intensity is likely modulated by storm structure, SST, moisture environment, land interaction, and mid-latitude circulation, which require process-based analyses beyond the scope of the present study.

https://doi.org/10.5194/egusphere-2026-3205
Preprint. Discussion started: 21 July 2026
© Author(s) 2026. CC BY 4.0 License.

4 Discussion

4.1 Distinguishing features relative to prior studies

This study proposes the CKLT framework as an observation-based analytical approach for treating typhoon cases that sequentially affect China and Korea within official national operational records as linked transboundary hazard processes. Previous East Asian typhoon studies have primarily focused on occurrence frequency, landfall characteristics, and hazard impacts within individual national domains (Ren et al., 2006; Na and Jung, 2020, 2024), whereas the sequential transboundary impact structure itself has received limited quantitative attention. By linking the CMA W8 station record and the KMA advisory record through the common WNP typhoon numbering system, this study analyses East Asian typhoon hazards as connected sequential impact events rather than as independent national records alone.

This statistical framework is intended as an observational foundation rather than a substitute for mechanistic investigation. The asymmetric long-term trends identified in this study — increasing China-affecting frequency in the CMA record, weakening station-based Chinese wind-related indicators, and intensifying advisory-based Korean extreme gust and typhoon-conditional precipitation indicators without a significant increase in Korea-affecting frequency in the KMA record — are difficult to fully characterise within single-country analytical frameworks and motivate the CKLT perspective. The distinguishable FW distributional structure further suggests that CKLT cases have distinct population-level statistical characteristics beyond a purely descriptive categorisation.

4.2 Statistical support for CKLT identification

The 36 identified CKLT cases recur throughout the 70 yr record, indicating that China–Korea sequential impacts are a recurrent pattern in the WNP typhoon record rather than isolated events. The choice of the FW $\leq$ 14 d threshold is supported by multiple lines of statistical evidence: GMM decomposition separates short- and long-FW components with a crossing point near 26.7 d, KDE indicates a local density minimum near 14–16 d, and sensitivity analysis across threshold values from 5 to 30 d yields a relatively stable range of 12–19 d with 33–37 CKLT cases. The convergence of these three independent criteria supports the use of 14 d as an inclusive upper bound rather than an arbitrary choice, and indicates that CKLT identification is not highly sensitive to the exact threshold chosen. The typhoon tracks provide additional physical consistency, showing a common north-eastward sequential structure from south-eastern China and the East China Sea–Yellow Sea corridor toward the Korean Peninsula across FW bins, with interpretable differences in recurvature tendency by FW category.

4.3 Operational implications of the Forecast Window for cross-border disaster risk reduction

The median FW of 6 d provides a useful reference for the population-level probabilistic timing of sequential China–Korea typhoon impacts. WNP numerical typhoon forecasts are generally considered most skillful within approximately 3–5 d of lead time, and observed China impact information may provide complementary observation-based timing information at lead times that are broadly comparable to, and in some cases extend beyond, the most skillful numerical range. Importantly, the CKLT

https://doi.org/10.5194/egusphere-2026-3205
Preprint. Discussion started: 21 July 2026
© Author(s) 2026. CC BY 4.0 License.

framework is not intended to replace numerical forecast systems. Rather, it may serve as a complementary observation-based indicator that supports earlier situational awareness of potential subsequent impacts at the regional scale.

The FW should be interpreted as a population-level probabilistic risk-timing indicator rather than a deterministic forecast of individual typhoon impacts. When CKLT-type impacts are identified along the Chinese coast, the framework may help inform preparatory awareness for potential subsequent wind and typhoon-conditional precipitation hazards in Korea, while recognising that actual hazard intensity at the individual-event level is governed by storm structure, SST, moisture environment, land interaction, and mid-latitude circulation. This perspective may be particularly relevant for sectors that require extended preparation time, including critical infrastructure protection, disaster response resource staging, port and logistics operations, and agricultural damage reduction.

From a disaster risk reduction (DRR) perspective, the recurrent China-to-Korea sequential structure documented here may be relevant for cross-border early warning communication, civil protection resource staging, and critical infrastructure preparedness in East Asia. Operational typhoon advisories are currently issued nationally, and CKLT-type sequential impacts are not formally accounted for in current bilateral early warning practice. An observation-based probabilistic timing indicator such as the FW can complement numerical guidance during the lead-time window before a typhoon enters the Korean emergency zone, particularly for sectors that require extended preparation time. Integrating CKLT-type information into existing World Meteorological Organization (WMO) and ESCAP Typhoon Committee operational frameworks is identified as a practical avenue for future trans-agency coordination research. Future work should quantitatively characterise the operationally available lead time between CMA impact onset and KMA special advisory issuance for confirmed CKLT cases and benchmark this lead time against the skillful range of current WNP numerical typhoon guidance.

4.4 Possible physical interpretations and future research

The asymmetric hazard pattern identified in Sects. 3.2 and 4.1 — weakening station-based mean wind-related indicators over China alongside increasing advisory-based extreme gust and typhoon-conditional precipitation indicators over Korea — may reflect several underlying physical processes. Because this study is based on 70 yr observational statistics and does not include ERA5-based composite analysis, the following hypotheses are explicitly framed as targets for future quantitative validation rather than established conclusions.

Hypothesis 1: path-dependent marine heat and moisture supply. Typhoons traversing the China coast and Yellow Sea may undergo dynamical weakening through surface friction and land–sea boundary interactions. Nevertheless, rapid recent SST warming in the East China Sea and the seas surrounding the Korean Peninsula (Han et al., 2023; Kim et al., 2024) may help maintain moisture supply along the transit path. Together with increasing atmospheric water vapour following the Clausius–Clapeyron relationship (Stansfield and Reed, 2023), this environment may contribute to enhanced precipitation-related hazard characteristics even when dynamical wind indicators weaken.

Hypothesis 2: precipitation structure modification during extratropical transition. Extratropical transition as typhoons approach the Korean Peninsula may expand and reorganise the precipitation field through interactions with frontal zones and mid-

https://doi.org/10.5194/egusphere-2026-3205
Preprint. Discussion started: 21 July 2026
© Author(s) 2026. CC BY 4.0 License.

latitude baroclinicity. In some cases, slower translation or quasi-stationary rainband structures may further concentrate precipitation over specific regions, contributing to increased accumulated precipitation over Korea. These hypotheses should be evaluated through ERA5-based CKLT composite analysis and high-resolution numerical experiments.

4.5 Limitations and future directions

This study has several limitations. First, regarding the long-term stationarity of the CMA observational network: the W8 dataset is based on fixed-station Bft ≥ 8 records, and the network expanded gradually over 1949–2018 rather than remaining strictly constant. We tested whether this expansion could account for the increasing China-affecting frequency trend reported in Sect. 3.1 through two complementary analyses (Sect. 2.1). The number of CMA stations actually contributing to the W8 record each year shows no significant long-term trend (Mann–Kendall $p = 0.37$), and a constant-network subset using only the 22 stations operational during 1949–1955 yields a Sen's slope of + 0.45 events decade^{-1} (Mann–Kendall $p = 0.032$), still positive and statistically significant. The W8 criterion is intensity-based (sustained wind ≥ 17.2 m s^{-1}), so a newly added station contributes to the impact record only when it observes Beaufort-8 winds during a passing typhoon, which is a stricter requirement than mere station existence. Together, these analyses indicate that network expansion does not account for the headline frequency increase, although the absolute magnitude of the trend may still be modulated by gradual densification of the inland and northern observational network. We caution that the asymmetric pattern between the CMA and KMA records (Sect. 3.2) and the CKLT identification (Sect. 3.3) do not depend on the absolute magnitude of the China-affecting frequency trend.
Second, JMA Best Track data prior to the satellite era, before approximately 1977, may carry larger position uncertainty, potentially affecting CKLT identification for early cases. Third, because this study focuses on long-term statistical characteristics, atmosphere–ocean interaction processes in individual CKLT cases are not directly analysed. The non-significant linear relationship between FW and Korea typhoon-conditional precipitation ($r = -0.08$, $p = 0.643$) supports the interpretation that CKLT precipitation characteristics are governed by multiple environmental factors rather than FW magnitude alone. Fourth, the reported Korea precipitation increase represents typhoon-conditional accumulated precipitation per event and is not separated here from broader regional precipitation changes. Disentangling typhoon-specific changes from background precipitation trends will require dedicated event-attribution analysis.

Finally, the CKLT sample size is relatively limited ($n = 36$). The gamma fit (KS $p = 0.258$) indicates that the observed FW distribution is statistically consistent with a parsimonious gamma model, and bootstrap resampling ($B = 5000$) suggests that the week-scale central tendency of the FW is stable under resampling, with the implied median FW within [2.95, 6.78] d. We adopt the gamma model as a simple and physically plausible parametric description for a non-negative right-skewed waiting-time variable rather than as the uniquely correct distributional form; other right-skewed distributions could provide comparable fits over the observed range and should be examined as the CKLT sample expands. Uncertainty remains for tail behaviour and for the long-FW component (FW > 14 d). Re-fitting the FW distribution with extended records and independent case identifications remains an important direction for further validation.

https://doi.org/10.5194/egusphere-2026-3205
Preprint. Discussion started: 21 July 2026
© Author(s) 2026. CC BY 4.0 License.

Future work will pursue ERA5-based CKLT composite analysis, high-resolution numerical experiments to examine physical mechanisms, and extension of the CKLT framework to include Japan, the Philippines, and the broader East Asian domain. These efforts would contribute to a more integrated basis for transboundary typhoon hazard assessment and observation-based probabilistic early warning.

5 Conclusions

This study examined long-term changes in typhoon hazards affecting China and Korea during 1949–2018 and proposed the China–Korea Linked Typhoon (CKLT) framework to identify the sequential impact structure in which the same WNP typhoon affects both countries in succession. The principal findings are as follows.

(1) Regional divergence in frequency trends. China-affecting typhoon frequency as recorded by the CMA W8 station network increased significantly (+ 0.570 events decade^{-1}, $p = 0.006$), and the ratio of China-affecting typhoons to total WNP genesis also showed a significant increasing trend (+ 0.022 decade^{-1}, $p = 0.003$), whereas Korea-affecting typhoon frequency in the KMA advisory record showed no significant long-term change. Total WNP typhoon genesis did not show a significant increasing trend. These results indicate that operationally documented regional typhoon impact frequency can evolve differently from basin-wide WNP genesis activity, and that a growing proportion of WNP typhoons has been documented as affecting China over the study period in the operational record. The China-affecting frequency trend remains positive and statistically significant when computed from a constant-network subset of stations operational since 1949–1955 (+ 0.45 events decade^{-1}, $p = 0.032$; Sect. 4.5), indicating that observational-network expansion does not account for the headline frequency increase.

(2) Asymmetric changes in operationally documented hazard indicators. Station-based mean maximum wind speed and mean maximum gust of China-affecting typhoons in the CMA W8 record decreased significantly, whereas Korea-affecting typhoons in the KMA advisory record showed increasing trends in advisory-based annual extreme gust and typhoon-conditional precipitation indicators. These contrasting trends indicate that operationally documented typhoon hazard indicators can show different long-term behaviour across neighbouring East Asian impact domains even when captured through different observational protocols; direct absolute comparisons remain constrained by differences in CMA and KMA operational definitions.

(3) CKLT identification and Forecast Window characteristics. Applying the three CKLT criteria — same WNP typhoon number, China impact precedence, and FW ≤ 14 d — identified 36 CKLT cases, representing 15.9 % of Korea-affecting typhoons in the KMA advisory record. GMM decomposition, KDE analysis, and threshold-sensitivity tests support the use of FW ≤ 14 d as a conservative upper bound for identifying linked events. For the confirmed CKLT cases, the FW distribution was adequately represented by a parsimonious gamma model ($\alpha = 1.20$, $\beta = 5.21$; KS $p = 0.258$), with a point-estimate median of 6 d. Bootstrap resampling indicated that the week-scale central tendency of the FW was stable under resampling, with an implied median FW confidence interval of [2.95, 6.78] d. With $n = 36$, the gamma form is adopted as a parsimonious working

https://doi.org/10.5194/egusphere-2026-3205
Preprint. Discussion started: 21 July 2026
© Author(s) 2026. CC BY 4.0 License.

model consistent with the non-negative, right-skewed support of the variable rather than as a uniquely identified generating distribution; other right-skewed distributions could provide comparable fits and should be re-examined as the CKLT sample expands.

Overall, these findings support the interpretation of East Asian typhoon hazards as transboundary sequential processes rather than independent national events alone. The CKLT framework provides an observational basis for identifying China–Korea linked typhoon impacts and characterising their population-level statistical timing. Observed China impact information may therefore inform the planning timescale used by Korean disaster-response authorities for subsequent Korea-related typhoon risk, but the population-level FW should not be interpreted as a deterministic forecast of individual storm impacts. Demonstrating an operational lead-time benefit relative to current advisory practice is beyond the scope of this study. Future work should extend this framework using ERA5-based composite analysis, high-resolution numerical experiments, and independent operational warning records to clarify the physical mechanisms and operational applicability of CKLT-type events.

Code and data availability

The JMA RSMC Tokyo best-track data (Japan Meteorological Agency, 2019) are openly distributed through the JMA website. The CMA Beaufort-8 station-based typhoon impact records and the KMA official typhoon impact list (1949−2018) were obtained from the respective agencies under data-use agreements that do not permit redistribution of the source files; researchers wishing to use these records should apply to the CMA and KMA directly. The CKLT case list compiled in this study, the data behind the figures, and the Python code used for the analysis are archived on Zenodo (Na and Jung, 2026a, b). Together they reproduce the case identification, the Mann−Kendall trend results, and the gamma-distribution fits reported in this paper.

Author contributions

HN and W-SJ conceptualised the study and designed the CKLT framework. HN curated the CMA, KMA, and JMA datasets, performed the formal analysis, developed the analysis code, produced the figures, and wrote the original draft. W-SJ supervised the work, acquired the funding, contributed to methodological design, and reviewed and edited the manuscript. Both authors have read and approved the final version.

Competing interests

The authors declare that they have no conflict of interest.

https://doi.org/10.5194/egusphere-2026-3205
Preprint. Discussion started: 21 July 2026
© Author(s) 2026. CC BY 4.0 License.

Disclaimer

Publisher's note: Copernicus Publications remains neutral with regard to jurisdictional claims made in the text, published maps, institutional affiliations, or any other geographical representation in this paper. While Copernicus Publications makes every effort to include appropriate place names, the final responsibility lies with the authors.

Acknowledgements

The authors thank the China Meteorological Administration (CMA), the Korea Meteorological Administration (KMA), and the Japan Meteorological Agency (JMA) for providing the tropical cyclone best-track and surface observation datasets that made this study possible. The authors also acknowledge the constructive feedback from colleagues at the Mesoscale Atmospheric and Air Quality Modeling Laboratory during the preparation of the manuscript.

Use of AI tools

During the preparation of this work, the authors used Claude (Anthropic) for English language editing. After using this tool, the authors reviewed and edited the content as needed and took full responsibility for the content of the publication.

Financial support

This research has been supported by the National Research Foundation of Korea (NRF) grant funded by the Ministry of Science and ICT of the Republic of Korea (grant no. RS-2023-00212688).

References

Brett, L., Bloomfield, H. C., Bradley, A., Calvet, T., Champion, A., De Angeli, S., de Ruiter, M. C., Guerreiro, S. B., Hillier, J., Jaroszweski, D., Kamranzad, B., Keinänen-Toivola, M. M., Kornhuber, K., Küpfer, K., Manning, C., Mattu, K., Murtagh, E., Murray, V., Ní Bhreasail, Á., O'Loughlin, F., Parker, C., Pregnolato, M., Ramos, A. M., Schlumberger, J., Theochari, D., Ward, P., Wessels, A., and White, C. J.: Science–policy–practice insights for compound and multi-hazard risks, Meteorol. Appl., 32, e70043, https://doi.org/10.1002/met.70043, 2025.

Efron, B. and Tibshirani, R. J.: An Introduction to the Bootstrap, Chapman and Hall/CRC, New York, USA, 436 pp., ISBN 9780412042317, 1993.

Emanuel, K.: Increasing destructiveness of tropical cyclones over the past 30 years, Nature, 436, 686–688, https://doi.org/10.1038/nature03906, 2005.

Hamed, K. H. and Rao, A. R.: A modified Mann–Kendall trend test for autocorrelated data, J. Hydrol., 204, 182–196, https://doi.org/10.1016/S0022-1694(97)00125-X, 1998.

Han, I.-S., Lee, J.-S., and Jung, H.-K.: Long-term pattern changes of sea surface temperature during summer and winter due to climate change in the Korea Waters, Fish. Aquat. Sci., 26, 639–648, https://doi.org/10.47853/FAS.2023.e43, 2023.

Japan Meteorological Agency: RSMC Tokyo-Typhoon Center Best Track Data, Japan Meteorological Agency [data set], https://www.jma.go.jp/jma/jma-eng/jma-center/rsmc-hp-pub-eg/besttrack.html (last access: 11 May 2026), 2019.

Kendall, M. G.: Rank Correlation Methods, 4th edn., Charles Griffin, London, UK, 202 pp., ISBN 9780852641996, 1975.

Kim, Y.-H., Min, S.-K., Son, S.-W., Choi, J., Seong, M.-G., and Zhang, X.: Global warming-induced warmer surface water over the East China Sea can intensify typhoons like Hinnamnor, B. Am. Meteorol. Soc., 105, E1416–E1421, https://doi.org/10.1175/BAMS-D-23-0240.1, 2024.

Kooshki Forooshani, M., van den Homberg, M., Kalimeri, K., Kaltenbrunner, A., Mejova, Y., Milano, L., Ndirangu, P., Paolotti, D., Teklesadik, A., and Turner, M. L.: Towards a global impact-based forecasting model for tropical cyclones, Nat. Hazards Earth Syst. Sci., 24, 309–329, https://doi.org/10.5194/nhess-24-309-2024, 2024.

Kossin, J. P., Emanuel, K. A., and Vecchi, G. A.: The poleward migration of the location of tropical cyclone maximum intensity, Nature, 509, 349–352, https://doi.org/10.1038/nature13278, 2014.

Liu, K. S. and Chan, J. C. L.: Growing threat of rapidly intensifying tropical cyclones in East Asia, Adv. Atmos. Sci., 39, 222–234, https://doi.org/10.1007/s00376-021-1126-7, 2022.

Mann, H. B.: Nonparametric tests against trend, Econometrica, 13, 245–259, https://doi.org/10.2307/1907187, 1945.

McLachlan, G. J. and Peel, D.: Finite Mixture Models, Wiley, New York, USA, 419 pp., ISBN 9780471006268, 2000.

Na, H. and Jung, W.-S.: Statistical characteristics of typhoons affecting the Korean Peninsula (1949–2018), Atmosphere, 11, 1062, https://doi.org/10.3390/atmos11101062, 2020.

Na, H. and Jung, W.-S.: Long-term trend analysis of typhoon characteristics over the Korean Peninsula using multi-source observational data, Atmosphere, 15, 287, https://doi.org/10.3390/atmos15030287, 2024.

Na, H. and Jung, W.-S.: CKLT processed case list and figure plot data (1949–2018), Zenodo [data set], https://doi.org/10.5281/zenodo.20509810, 2026a.

Na, H. and Jung, W.-S.: CKLT analysis code (Python) for China–Korea Linked Typhoon identification and statistical analysis, Zenodo [code], https://doi.org/10.5281/zenodo.20509869, 2026b.

https://doi.org/10.5194/egusphere-2026-3205
Preprint. Discussion started: 21 July 2026
© Author(s) 2026. CC BY 4.0 License.

Raymond, C., Horton, R. M., Zscheischler, J., Martius, O., AghaKouchak, A., Balch, J., Bowen, S. G., Camargo, S. J., Hess, J., Kornhuber, K., Oppenheimer, M., Ruane, A. C., Wahl, T., and White, K.: Understanding and managing connected extreme events, Nat. Clim. Change, 10, 611–621, https://doi.org/10.1038/s41558-020-0790-4, 2020.

Ren, F., Wu, G., Dong, W., Wang, X., Wang, Y., Ai, W., and Li, W.: Changes in tropical cyclone precipitation over China, Geophys. Res. Lett., 33, L20702, https://doi.org/10.1029/2006GL027951, 2006.

Sen, P. K.: Estimates of the regression coefficient based on Kendall's tau, J. Am. Stat. Assoc., 63, 1379–1389, https://doi.org/10.1080/01621459.1968.10480934, 1968.

Silverman, B. W.: Density Estimation for Statistics and Data Analysis, Chapman and Hall, London, UK, 175 pp., ISBN 9780412246203, 1986.

Stansfield, A. M. and Reed, K. A.: Global tropical cyclone precipitation scaling with sea surface temperature, npj Clim. Atmos. Sci., 6, 60, https://doi.org/10.1038/s41612-023-00391-6, 2023.

UNDRR: Sendai Framework for Disaster Risk Reduction 2015–2030, United Nations Office for Disaster Risk Reduction, Geneva, Switzerland, 37 pp., https://www.undrr.org/publication/sendai-framework-disaster-risk-reduction-2015-2030 (last access: 2 June 2026), 2015.

Webster, P. J., Holland, G. J., Curry, J. A., and Chang, H.-R.: Changes in tropical cyclone number, duration, and intensity in a warming environment, Science, 309, 1844–1846, https://doi.org/10.1126/science.1116448, 2005.

Wilks, D. S.: Statistical Methods in the Atmospheric Sciences, 3rd edn., Academic Press, Oxford, UK, 704 pp., ISBN 9780123850225, 2011.

Ying, M., Zhang, W., Yu, H., Lu, X., Feng, J., Fan, Y., Zhu, Y., and Chen, D.: An overview of the China Meteorological Administration tropical cyclone database, J. Atmos. Ocean. Tech., 31, 287–301, https://doi.org/10.1175/JTECH-D-12-00119.1, 2014.

Yue, S. and Wang, C.: The Mann–Kendall test modified by effective sample size to detect trend in serially correlated hydrological series, Water Resour. Manage., 18, 201–218, https://doi.org/10.1023/B:WARM.0000043140.61082.60, 2004.

Zscheischler, J., Westra, S., van den Hurk, B. J. J. M., Seneviratne, S. I., Ward, P. J., Pitman, A., AghaKouchak, A., Bresch, D. N., Leonard, M., Wahl, T., and Zhang, X.: Future climate risk from compound events, Nat. Clim. Change, 8, 469–477, https://doi.org/10.1038/s41558-018-0156-3, 2018.

Zscheischler, J., Martius, O., Westra, S., Bevacqua, E., Raymond, C., Horton, R. M., van den Hurk, B., AghaKouchak, A., Jézéquel, A., Mahecha, M. D., Maraun, D., Ramos, A. M., Ridder, N. N., Thiery, W., and Vignotto, E.: A typology of compound weather and climate events, Nat. Rev. Earth Environ., 1, 333–347, https://doi.org/10.1038/s43017-020-0060-z, 2020.